UNIVERSITY OF AMSTERDAM

UvA-DARE (Digital Academic Repository)

Exploiting the Hermitian symmetry in tensor network algorithms

van Alphen, Oscar; Kleijweg, Stijn V.; Hasik, Juraj; Corboz, Philippe

DOI
10.48550/arXiv.2410.11596
10.1103/PhysRevB.111.045105

Publication date
2025

Document Version
Author accepted manuscript

Published in
Physical Review B

Link to publication

Citation for published version (APA):
van Alphen, O., Kleijweg, S. V., Hasik, J., & Corboz, P. (2025). Exploiting the Hermitian symmetry in tensor network algorithms. *Physical Review B*, *111*(4), Article 045105. https://doi.org/10.48550/arXiv.2410.11596, https://doi.org/10.1103/PhysRevB.111.045105

General rights
It is not permitted to download or to forward/distribute the text or part of it without the consent of the author(s) and/or copyright holder(s), other than for strictly personal, individual use, unless the work is under an open content license (like Creative Commons).

Disclaimer/Complaints regulations
If you believe that digital publication of certain material infringes any of your rights or (privacy) interests, please let the Library know, stating your reasons. In case of a legitimate complaint, the Library will make the material inaccessible and/or remove it from the website. Please Ask the Library: https://uba.uva.nl/en/contact, or a letter to: Library of the University of Amsterdam, Secretariat, P.O. Box 19185, 1000 GD Amsterdam, The Netherlands. You will be contacted as soon as possible.

UvA-DARE is a service provided by the library of the University of Amsterdam (https://dare.uva.nl)

Download date:10 Oct 2026

Exploiting the Hermitian symmetry in tensor network algorithms

Oscar van Alphen,[1] Stijn V. Kleijweg,[1] Juraj Hasik,[1,2] and Philippe Corboz[1]

[1] *Institute for Theoretical Physics, University of Amsterdam, Science Park 904, 1098 XH Amsterdam, The Netherlands*

[2] *Department of Physics, University of Zurich, Winterthurerstrasse 190, 8057 Zurich, Switzerland*

Exploiting symmetries in tensor network algorithms plays a key role for reducing the computational and memory costs. Here we explain how to incorporate the Hermitian symmetry in double-layer tensor networks, which naturally arise in methods based on projected entangled-pair states (PEPS). For real-valued tensors the Hermitian symmetry defines a $\mathbb{Z}_2$ symmetry on the combined bra and ket auxiliary level of the tensors. By implementing this symmetry, a speedup of the computation time by up to a factor 4 can be achieved, while expectation values of observables and reduced density matrices remain Hermitian by construction. Benchmark results based on the corner transfer matrix renormalization group (CTMRG) and higher-order tensor renormalization group (HOTRG) are presented. We also discuss how to implement the Hermitian symmetry in the complex case, where a similar speedup can be achieved.

arXiv:2410.11596v2 [cond-mat.str-el] 24 Jan 2025

I. INTRODUCTION

Tensor networks offer highly accurate numerical tools for the study of strongly-correlated systems, in particular in cases where Monte Carlo methods are ineffective due to the negative sign problem. Most notably, matrix product states have revolutionized the study of quasi-one dimensional systems [1, 2]. Their higher dimensional generalization, known as projected entangled-pair states (PEPS) [3–5], have become a state-of-the-art tool for two dimensional systems, with applications ranging from frustrated magnets to strongly correlated electron systems, see e.g. Refs. [6–33]. The main idea is to efficiently represent quantum many-body states by a contraction of tensors, where the accuracy is systematically controlled by the bond dimension D of the tensors.

A central ingredient to speeding up tensor network calculations is exploiting global symmetries of the states, such as the U(1) symmetry for systems that conserve the total number of particles [34, 35], or non-abelian SU(2) symmetry in certain spin models [36–39]. In the presence of a global symmetry, the tensors can be written in block-sparse form, where the blocks are labeled by the corresponding quantum numbers (e.g. different particle number sectors), and tensor contractions decompose into a product of several smaller blocks, similar to the multiplication of block diagonal matrices, enabling a substantial reduction in computational cost. Another important direction is classifying exotic phases of matter according to the symmetry properties of the tensors in their auxiliary space [40–45].

In this paper we consider a different symmetry inherent to standard tensor network calculations, namely the Hermitian symmetry of double-layer networks representing, e.g., the norm of a state or a reduced density matrix (RDM) in the physical (or auxiliary) space. An RDM computed from an MPS is always Hermitian up to machine precision. However, for PEPS, since the contraction is typically done only approximately, the contraction error can lead to violations of the Hermiticity of RDMs. Here we show how to explicitly preserve the Hermiticity by working in a symmetric basis of the combined bra and ket auxiliary space. In the case of real-valued tensors, the Hermitian symmetry corresponds to a $\mathbb{Z}_2$ symmetry which can be implemented in the standard way [34, 35], or by making use of symmetric tensor libraries [46–59].

The main benefit, besides preserving Hermiticity, is a roughly fourfold speedup in computation time and a twofold reduction in memory. As a proof of concept, we present benchmark results based on two standard contraction methods: the corner transfer-matrix renormalization group (CTMRG) [60] and the higher-order tensor renormalization group (HOTRG) [61]. We also discuss the complex-valued case, which does not lead to a regular block-sparse form of a tensor, but results in a block-sparse structure for the real and complex parts individually. By exploiting this structure, a similar speedup can be achieved.

II. METHOD

A. iPEPS ansatz and contraction

We consider a translationally invariant infinite PEPS (iPEPS) [5] which represents a 2D wave function in the thermodynamic limit. It consists of a rank-5 tensor A repeated on a square lattice as shown in Fig. 1(a). Each tensor has 4 auxiliary legs with bond dimension D connecting the neighboring tensors and one physical leg with the dimension d of the local Hilbert space of a lattice site. Combining each tensor A with its conjugate $A^\dagger$ into a new tensor a (Fig. 1(b)) results in a square lattice tensor network shown in Fig. 1(c), representing the norm of the wave function.

To approximately contract the network, we use CTMRG [60] and HOTRG [61], where the accuracy is controlled by the bond dimension χ. In CTMRG, the system with open boundary conditions is grown in all four directions by iteratively absorbing rows and columns

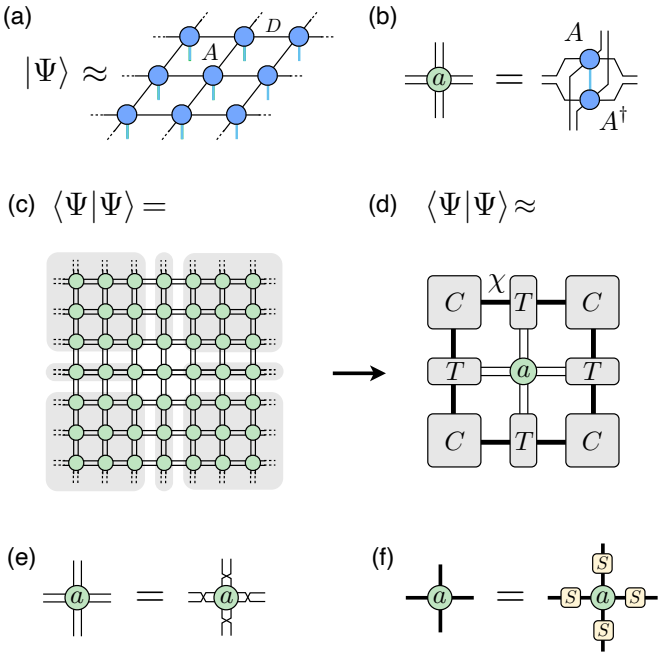

FIG. 1. (a) Translationally invariant iPEPS parametrized by a tensor A with bond dimension D. The vertical blue legs represent the physical indices on each lattice site. (b) The double-layer tensor a is defined as the contraction of A with $A^\dagger$ along the physical leg. (c) Representation of the norm in terms of the a tensors. (d) In CTMRG the tensor network surrounding the center tensor a is approximated by four corner (C) and edge (T) environment tensors, where the accuracy of the approximate contraction is controlled by the bond dimension χ. (e) For real-valued tensors, a is invariant under the exchange of all ket legs with bra legs. (f) The bra and ket indices can be combined into a bigger index of bond dimension D^2. S represents the swap operation of bra and ket legs shown in (e).

of the network into the boundary tensors with bond dimension χ. Each iteration increases the boundary bond dimension by a factor D^2, which is truncated down to χ based on an eigenvalue or singular value decomposition (SVD) [60]. The boundary tensors consist of four corner tensors C and four edge tensors T, representing a quarter infinite system or an infinite half-row or half-column of tensors, see Fig. 1(d). For simplicity, we consider translationally invariant states with a $C4v$ symmetry such that all corners and edges are equivalent. HOTRG is based on iteratively coarse-graining the lattice of tensors. At each iteration, two neighboring a tensors are combined into one tensor (alternating between bra and ket horizontal and vertical direction), followed by a truncation down to the χ most relevant states based on an eigenvalue decomposition (or SVD) [61].

B. $\mathbb{Z}_2$ symmetry in the real-valued case

Let us consider the combined bra and ket tensor PEPS in Fig. 1(b). If we take the tensor A to be real valued, the bra and ket tensors are equal, i.e. $A = A^\dagger$, and the double-layer tensor $a_{i\bar{i}j\bar{j}k\bar{k}l\bar{l}}$ is invariant under the simultaneous exchange of all bra and ket indices, i.e. $a_{i\bar{i}j\bar{j}k\bar{k}l\bar{l}} = a_{\bar{i}i\bar{j}j\bar{k}k\bar{l}l}$, as depicted in Fig. 1(e). The swapping of the legs can also be represented as a swap tensor S, defined as $S_{i\bar{i}j\bar{j}} = \delta_{i\bar{j}}\delta_{\bar{i}j}$.

By combining each pair of virtual indices on the bra and ket level into one big index of bond dimension D^2, we can represent tensor a as a four-legged tensor shown in Fig. 1(e). In this combined basis S becomes a $D^2 \times D^2$ matrix acting on a joint leg, and acting with S on all four legs of a simultaneously leaves the tensor a invariant (Fig. 1(f)). Since $S^2 = \mathbb{I}$, S defines a $\mathbb{Z}_2$ symmetry for tensor a.

As with other symmetries, if we represent the tensor a in the eigenbasis of S, the tensor acquires a block-sparse structure, where the blocks can be labelled by the eigenvalues of S, which are either $+1$ (even) or -1 (odd). For example for $D = 2$, starting from the combined basis of the bra and ket virtual index $\{(1\bar{1}), (2\bar{1}), (1\bar{2}), (2\bar{2})\}$, the eigenbasis of S is given by $\{(1\bar{1}), (2\bar{2}), (1\bar{2} + 2\bar{1})/\sqrt{2}, (1\bar{2} - 2\bar{1})/\sqrt{2}\}$, where the first three states belong to the even sector (eigenvalue +1) and the last state to the odd sector (eigenvalue -1). One can easily show that for a given D the even sector has dimension $dim(even) = D + (D^2 - D)/2$ and $dim(odd) = (D^2 - D)/2$. This is because there are D even basis states of the form $(k\bar{k})$, and half of the remaining states is a symmetric combination $(k\bar{l} + l\bar{k})/\sqrt{2}$, the other half an antisymmetric combination $(k\bar{l} - l\bar{k})/\sqrt{2}$, with $k \neq l$, respectively.

Working in the eigenbasis of S has three advantages. (1) Thanks to the block-sparse structure of the tensors, the computational cost to contract two tensors or to perform an SVD of a tensor is lower than in the dense case. (2) The block-sparse structure can also be exploited to reduce the memory cost, by storing only the blocks which are non-zero. (3) The tensor a retains its symmetry also when the virtual space is truncated to a lower bond dimension. The latter is not the case in the non-symmetric basis. For example, for $D = 2$ when keeping only the first two basis states $\{(1\bar{1}), (2\bar{1})\}$, the tensor a would no longer be Hermitian. Using tensors that break the physical Hermitian symmetry will result in non-physical quantities, e.g. any reduced density matrix computed from such tensors will not be Hermitian.

Having identified the underlying $\mathbb{Z}_2$ symmetry of tensor a, one can implement the symmetry as described in Refs. [34, 35] (or use a symmetric tensor library) to contract tensors and to perform operations on tensors like an SVD or an eigenvalue decomposition. What is different from the standard case of a physical global $\mathbb{Z}_2$ symmetry (like e.g. in the transverse field Ising model or parity conservation in fermionic systems), is that the even and odd

sectors can only be defined on the combined virtual bra and ket spaces (e.g. for a), but not on the individual bra and ket level (e.g. for A). As a consequence, for a multiplication of e.g. an a tensor with an A tensor, a dense contraction has to be performed, because the A tensor is not symmetric. Thus, for certain operations involving individual bra- or ket- tensors, the $\mathbb{Z}_2$ symmetry cannot be exploited. Still, typically the computationally most expensive calculations in 2D contraction algorithms are those involving only combined bra and ket spaces, e.g. the SVD in CTMRG's renormalization step or in essentially all steps in HOTRG (except in the initialization step in which the a tensor is formed, which is computationally subleading).

The maximal gain in computational cost is a factor 4, which is obtained if the sizes of the even and odd sectors are equal. This can be easily seen from the multiplication of two block-diagonal matrices of size $M \times M$. The computational cost of the dense multiplication scales as M^3. Multiplying two blocks of half of the size has a reduced cost of $2 \times (M/2)^3 = M^3/4$, hence a factor 4. For the a tensor $dim(even) = dim(odd)$ is asymptotically true in the infinite D limit. For the renormalized spaces in CTMRG and HOTRG, we will analyze the relative sizes of even and odd sectors in the results in Sec.III B. In practice, a factor 4 may not be achieved, even for $dim(even) = dim(odd)$, because keeping track of the sectors comes with a certain computational overhead (depending on the actual implementation), such that a factor 4 is only reached asymptotically in the large bond dimension limit.

We note that the Hermitian $\mathbb{Z}_2$ symmetry cannot be trivially combined with a global symmetry such as U(1) or SU(2). For example, consider the U(1) symmetry arising from conservation of the total S^z in a spin model. Here, the swap tensor S mixes different sectors of the total S^z [62]. One could in principle still implement the $\mathbb{Z}_2$ for the total $S^z = 0$ block, and exploit the fact that the $\mathbb{Z}_2$ Hermitian symmetry results in a block sparse structure, where the blocks in the total $S^z = k$ can be mapped onto blocks with total $S^z = -k$, so that it is sufficient to keep only the positive sectors. Thus, while profiting from the $\mathbb{Z}_2$ Hermitian symmetry is possible in this context, it would involve modifications in the underlying tensor library to deal with this particular case, which is beyond the scope of this work.

C. Hermitian symmetry in the complex case

For complex valued tensors, $A \neq A^\dagger$ and hence the a tensor is not invariant upon exchanging all bra and ket legs. The real part of a is invariant, but the imaginary part of a requires a minus sign due to the complex conjugation. One can nevertheless implement the Hermitian symmetry and obtain up to factor 4 speed up as we explain in the following.

We first recall that multiplying two complex numbers comes with a factor 4 compared to real numbers, because it involves 4 multiplications instead of only a single one, e.g. $(a+bi)(c+di) = ac - bd + (bc+ad)i$. Now, if we represent a in the eigenbasis of S it turns out that all the blocks in the total even sector are purely real valued, whereas all blocks in the total odd sector are purely imaginary. Thus, the a tensor is not block sparse, but it nevertheless has a block structure, where each block contains either only real numbers or imaginary numbers. As a consequence, when multiplying two matrices (or tensors) in the eigenbasis of S, all operations involve multiplications between purely real numbers and/or purely imaginary numbers requiring only a single multiplication per pair of numbers, hence there is a factor 4 reduction in computational cost. In addition, as in the real-valued case, working in the eigenbasis of S has the advantage that truncations on the virtual space will preserve the Hermitian symmetry of the tensor network.

Working with dense tensors with a block structure is typically not supported in standard symmetric libraries. However, one can still make use of standard libraries by using the following trick. Imagine we want to multiply two matrices (or tensors) b which exhibit such a block structure, but which are not block sparse. We can now add an extra leg of dimension 2 with index q to each tensor, resulting in a new tensor $\tilde{b}$, with $q = 1$ and $q = 2$ corresponding to the even and odd sector. We can then store the real part and imaginary part of b in the $q = 1$ and $q = 2$ slices, respectively,

$$\begin{aligned} \tilde{b}(:,:,1) &= \mathrm{Re}[b(:,:)], \\ \tilde{b}(:,:,2) &= \mathrm{Im}[b(:,:)]. \end{aligned} \tag{1}$$

The new tensor $\tilde{b}$ has purely real numbers and a block-sparse structure, i.e. it can be represented using a standard symmetric tensor library. The contraction of the two tensors involves an extra tensor f which combines the real and imaginary parts according to the multiplication rules of complex numbers, i.e.

$$\begin{aligned} f(1,1,1) &= 1, \quad f(2,2,1) = -1 \\ f(1,2,2) &= 1, \quad f(2,1,2) = 1, \end{aligned} \tag{2}$$

and the multiplication of two $\tilde{b}$ tensors then reads

$$\tilde{c}_{ikr} = \sum_{jpq} \tilde{b}_{ijp} \tilde{b}_{jkq} f_{pqr}. \tag{3}$$

Converting such a real-valued tensor back to a complex-valued one can simply be done by multiplying the extra leg by the vector $[1, i]$.

III. BENCHMARK RESULTS

In this section we present benchmark results for the contraction of the ground state of the Heisenberg model based on the converged tensors from Ref. [22], using

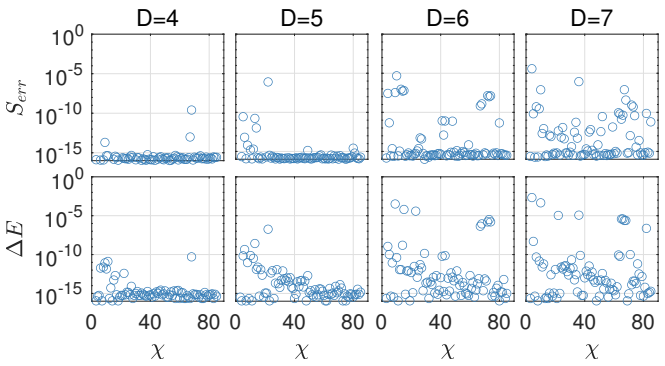

FIG. 2. Upper panels: Symmetry error in CTMRG as a function of χ for different bond dimensions D. Lower panels: Energy difference between the non-symmetric and $\mathbb{Z}_2$ symmetric implementation of CTMRG.

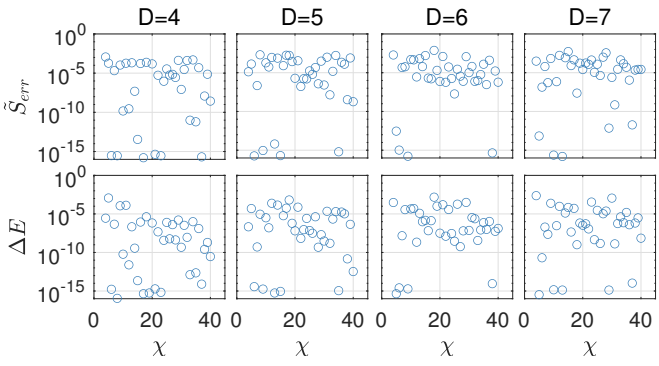

FIG. 3. Upper panels: Symmetry error in HOTRG as a function of χ for different bond dimensions D. Lower panels: Energy difference between the non-symmetric and $\mathbb{Z}_2$ symmetric implementation of HOTRG.

CTMRG and HOTRG with and without implemented $\mathbb{Z}_2$ symmetry. The lowest energy states for different bond dimensions D allow for a real-valued tensor network representation.

A. Hermitian symmetry error

As discussed in the previous section, in standard CTMRG and HOTRG the truncation performed during the contraction may be such that the Hermitian symmetry of the tensor network is lost, which may lead to unphysical results, such as non-Hermitian reduced density matrices. For CTMRG we define the following Hermitian symmetry error:

$$S_{err} = \frac{||\epsilon - \epsilon^\dagger||}{||\epsilon + \epsilon^\dagger||}, \tag{4}$$

where ϵ corresponds to Fig. 1(d) with the tensor a removed in the center, i.e. a one-site environment with four open auxiliary bonds on the bra and on the ket level, respectively. If the Hermitian symmetry is preserved during the CTMRG iterations, we should obtain $\epsilon = \epsilon^\dagger$ and hence $S_{err} = 0$. To measure the symmetry error in HOTRG, we replace one of the a tensors in the network by another tensor b which, when reshaped to a $D^4 \times D^4$ matrix, has 1's in the upper triangle and -1's in the lower triangle (and zeros on the diagonal). If the environment is Hermitian, the contraction yields zero, and hence deviations from zero imply a non-Hermitian environment. We normalize the error by a similar evaluation of the network using $|b|$, i.e. with all off-diagonal elements being 1 when reshaped to a matrix.

Figure 2 (upper panels) shows the symmetry error for the non-symmetric CTMRG as a function of χ and different values of D. For small bond dimension, the symmetry error vanishes for most values of χ. An increasing number of non-vanishing errors is obtained at larger D for specific values of χ, but their magnitudes remain relatively small.

Figure 2 (lower panels) shows the difference in energy between the symmetric and non-symmetric CTMRG, $\Delta E = |E_{sym} - E|$. We find that a finite S_{err} induces also a difference in energy. Sizable deviations of the order $\Delta E \sim 10^{-4} - 10^{-3}$ (in units of the Heisenberg exchange coupling J) can be found at large D and small χ. However, with increasing χ, the observed deviations become substantially smaller [63].

In Fig. 3 we present similar results obtained with HOTRG. The maximal deviation ΔE is of similar order as in the CTMRG case, however, symmetry errors are found to occur more frequently. One possible reason is that in CTMRG, a new bulk tensor a, which is perfectly symmetric, is absorbed into the environment at each iteration, which probably helps to preserve the symmetry in the environment up to a large extent. In HOTRG, however, only the initial tensor a in the first iteration is perfectly symmetric, whereas at later iterations two coarse-grained tensors are combined, such that symmetry errors can accumulate.

In both cases, implementing the $\mathbb{Z}_2$ Hermitian symmetry enables to keep the tensors perfectly symmetric, i.e. the symmetry error is zero by construction.

B. Computational speedup

In Fig. 4(a) we present results for the computational speedup for different values of D and χ, based on the average time of a CTMRG iteration. For small D and χ, the speedup factor is smaller than at large values. This is because the calculation with $\mathbb{Z}_2$ symmetric tensors comes with a certain overhead to permute and reshape the tensors. For larger tensors, this overhead becomes small compared to the time of the matrix-matrix multiplications or SVD, such that larger speedups can be achieved. This overhead could be further reduced by making use of a more efficient $\mathbb{Z}_2$ tensor class implementation.

Another factor which influences the time are the block sizes of the even and odd sectors. In Fig. 4(b) we can

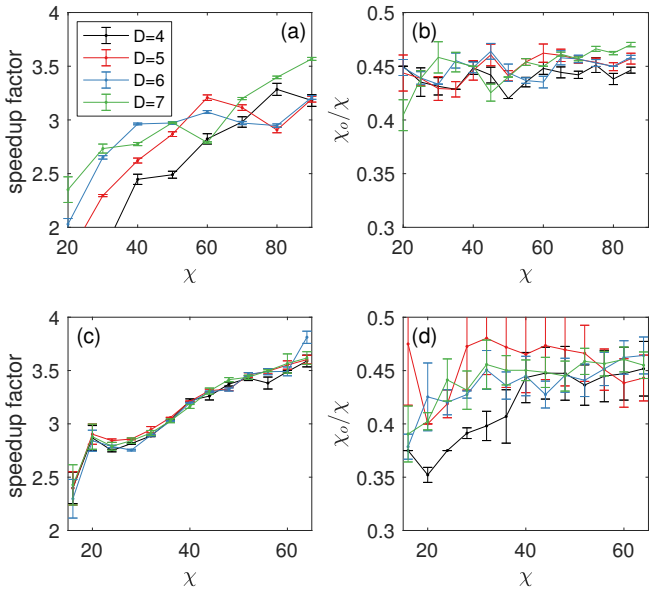

FIG. 4. Speedup factor between non-symmetric and symmetric CTMRG (a) and HOTRG (c) as a function of χ for different bond dimensions D. The corresponding average ratio of the even and odd sectors with the corresponding standard deviation is shown in (b) and (d), respectively.

see that the size of the odd sector is increasing with χ, with a value of around 47% for $D = 7, \chi = 100$ which is already close to optimal (i.e. 50%). In Fig. 4(c),(d) we present similar results for HOTRG. Also here we observe that the speedup factor approaches four with increasing χ. Here, the speedup factor is essentially independent of D, because D is only relevant in the first iteration in HOTRG.

IV. CONCLUSIONS

In this paper, we have shown how to incorporate the Hermitian symmetry in 2D tensor network contractions. In the case of real-valued tensors, the double-layer tensors exhibit a $\mathbb{Z}_2$ symmetry which can be implemented using standard symmetric tensor libraries. Exploiting this symmetry yields a speedup of up to a factor 4 in the large bond dimension limit, and the Hermitian symmetry of reduced density matrices is preserved by construction.

We also discussed the complex-valued case, where the tensors exhibit a block sparse structure for the real part and imaginary part separately, with the real (imaginary) numbers lying in the total even (odd) sector. Exploiting this structure reduces the number of operations by a factor 4, because tensor contractions involve multiplications between purely real numbers and/or purely imaginary numbers, instead of a multiplication of general complex numbers.

Besides CTMRG and HOTRG, our approach can be applied in various other context, e.g. in other 2D [64–70] or 3D contraction algorithms [71, 72], or to preserve the Hermiticity of density matrices in single-layer finite temperature algorithms [73] or in open-system time evolutions [74, 75].

ACKNOWLEDGMENTS

This project has received funding from the European Research Council (ERC) under the European Union's Horizon 2020 research and innovation programme (grant agreement No. 101001604). J.H. acknowledges support from the Swiss National Science Foundation through a Consolidator Grant (iTQC, TMCG-2 213805).

[1] S. R. White, Density matrix formulation for quantum renormalization groups, Phys. Rev. Lett. **69**, 2863 (1992).
[2] U. Schollwöck, The density-matrix renormalization group in the age of matrix product states, Annals of Physics **326**, 96 (2011).
[3] F. Verstraete and J. I. Cirac, Renormalization algorithms for Quantum-Many Body Systems in two and higher dimensions, arXiv:cond-mat/0407066 (2004).
[4] Y. Nishio, N. Maeshima, A. Gendiar, and T. Nishino, Tensor Product Variational Formulation for Quantum Systems, Preprint (2004), arXiv:cond-mat/0401115.
[5] J. Jordan, R. Orús, G. Vidal, F. Verstraete, and J. I. Cirac, Classical Simulation of Infinite-Size Quantum Lattice Systems in Two Spatial Dimensions, Phys. Rev. Lett. **101**, 250602 (2008).
[6] P. Corboz and F. Mila, Crystals of bound states in the magnetization plateaus of the Shastry-Sutherland model, Phys. Rev. Lett. **112**, 147203 (2014).
[7] P. Nataf, M. Lajkó, P. Corboz, A. M. Läuchli, K. Penc, and F. Mila, Plaquette order in the SU(6) Heisenberg model on the honeycomb lattice, Phys. Rev. B **93**, 201113 (2016).
[8] H. J. Liao, Z. Y. Xie, J. Chen, Z. Y. Liu, H. D. Xie, R. Z. Huang, B. Normand, and T. Xiang, Gapless Spin-Liquid Ground State in the $S = 1/2$ Kagome Antiferromagnet, Phys. Rev. Lett. **118**, 137202 (2017).
[9] I. Niesen and P. Corboz, Emergent Haldane phase in the $S = 1$ bilinear-biquadratic Heisenberg model on the square lattice, Phys. Rev. B **95**, 180404(R) (2017).
[10] J.-Y. Chen, L. Vanderstraeten, S. Capponi, and D. Poilblanc, Non-Abelian chiral spin liquid in a quantum antiferromagnet revealed by an iPEPS study, Phys. Rev. B **98**, 184409 (2018).
[11] H.-Y. Lee and N. Kawashima, Spin-one bilinear-biquadratic model on a star lattice, Phys. Rev. B **97**, 205123 (2018).
[12] S. S. Jahromi and R. Orús, Spin-$\frac{1}{2}$ Heisenberg antiferromagnet on the star lattice: Competing valence-bond-solid phases studied by means of tensor networks, Phys. Rev. B **98**, 155108 (2018).

[13] I. Niesen and P. Corboz, Ground-state study of the spin-1 bilinear-biquadratic Heisenberg model on the triangular lattice using tensor networks, Phys. Rev. B **97**, 245146 (2018).

[14] H. Yamaguchi, Y. Sasaki, T. Okubo, M. Yoshida, T. Kida, M. Hagiwara, Y. Kono, S. Kittaka, T. Sakakibara, M. Takigawa, Y. Iwasaki, and Y. Hosokoshi, Field-enhanced quantum fluctuation in an $S = \frac{1}{2}$ frustrated square lattice, Phys. Rev. B **98**, 094402 (2018).

[15] A. Kshetrimayum, C. Balz, B. Lake, and J. Eisert, Tensor network investigation of the double layer Kagome compound $Ca_{10}Cr_7O_{28}$, arXiv:1904.00028 [cond-mat, physics:quant-ph] (2019).

[16] S. S. Chung and P. Corboz, SU(3) fermions on the honeycomb lattice at $\frac{1}{3}$ filling, Phys. Rev. B **100**, 035134 (2019).

[17] B. Ponsioen, S. S. Chung, and P. Corboz, Period 4 stripe in the extended two-dimensional Hubbard model, Phys. Rev. B **100**, 195141 (2019).

[18] H.-Y. Lee, R. Kaneko, L. E. Chern, T. Okubo, Y. Yamaji, N. Kawashima, and Y. B. Kim, Magnetic field induced quantum phases in a tensor network study of Kitaev magnets, Nat. Comm. **11**, 1639 (2020).

[19] O. Gauthé, S. Capponi, M. Mambrini, and D. Poilblanc, Quantum spin liquid phases in the bilinear-biquadratic two-SU(4)-fermion Hamiltonian on the square lattice, Phys. Rev. B **101**, 205144 (2020).

[20] J. L. Jiménez, S. P. G. Crone, E. Fogh, M. E. Zayed, R. Lortz, E. Pomjakushina, K. Conder, A. M. Läuchli, L. Weber, S. Wessel, A. Honecker, B. Normand, C. Rüegg, P. Corboz, H. M. Rønnow, and F. Mila, A quantum magnetic analogue to the critical point of water, Nature **592**, 370 (2021).

[21] P. Czarnik, M. M. Rams, P. Corboz, and J. Dziarmaga, Tensor network study of the $m = \frac{1}{2}$ magnetization plateau in the Shastry-Sutherland model at finite temperature, Phys. Rev. B **103**, 075113 (2021).

[22] J. Hasik, D. Poilblanc, and F. Becca, Investigation of the Néel phase of the frustrated Heisenberg antiferromagnet by differentiable symmetric tensor networks, SciPost Physics **10**, 012 (2021).

[23] Z. Shi, S. Dissanayake, P. Corboz, W. Steinhardt, D. Graf, D. M. Silevitch, H. A. Dabkowska, T. F. Rosenbaum, F. Mila, and S. Haravifard, Discovery of quantum phases in the Shastry-Sutherland compound $SrCu_2(BO_3)_2$ under extreme conditions of field and pressure, Nat. Comm. **13**, 2301 (2022).

[24] W.-Y. Liu, J. Hasik, S.-S. Gong, D. Poilblanc, W.-Q. Chen, and Z.-C. Gu, Emergence of Gapless Quantum Spin Liquid from Deconfined Quantum Critical Point, Phys. Rev. X **12**, 031039 (2022).

[25] O. Gauthé and F. Mila, Thermal Ising Transition in the Spin-1/2 J_1-J_2 Heisenberg Model, Phys. Rev. Lett. **128**, 227202 (2022).

[26] M. Peschke, B. Ponsioen, and P. Corboz, Competing states in the two-dimensional frustrated kondo-necklace model, Phys. Rev. B **106**, 205140.

[27] J. Hasik, M. Van Damme, D. Poilblanc, and L. Vanderstraeten, Simulating Chiral Spin Liquids with Projected Entangled-Pair States, Phys. Rev. Lett. **129**, 177201 (2022).

[28] A. Sinha, M. M. Rams, P. Czarnik, and J. Dziarmaga, Finite-temperature tensor network study of the Hubbard model on an infinite square lattice, Phys. Rev. B **106**, 195105 (2022).

[29] B. Ponsioen, S. S. Chung, and P. Corboz, Superconducting stripes in the hole-doped three-band Hubbard model, Phys. Rev. B **108**, 205154 (2023).

[30] E. L. Weerda and M. Rizzi, Fractional quantum hall states with variational projected entangled-pair states: a study of the bosonic harper-hofstadter model, arXiv:2309.12811 (2023).

[31] Y. Xu, S. Capponi, J.-Y. Chen, L. Vanderstraeten, J. Hasik, A. H. Nevidomskyy, M. Mambrini, K. Penc, and D. Poilblanc, Phase diagram of the chiral SU(3) antiferromagnet on the kagome lattice, Phys. Rev. B **108**, 195153.

[32] J. Hasik and P. Corboz, Incommensurate Order with Translationally Invariant Projected Entangled-Pair States: Spiral States and Quantum Spin Liquid on the Anisotropic Triangular Lattice, Phys. Rev. Lett. **133**, 176502 (2024).

[33] P. Schmoll, J. Naumann, J. Eisert, and Y. Iqbal, Bathing in a sea of candidate quantum spin liquids: From the gapless ruby to the gapped maple-leaf lattice, arXiv:2407.07145 [cond-mat] (2024).

[34] S. Singh, R. N. C. Pfeifer, and G. Vidal, Tensor network states and algorithms in the presence of a global U(1) symmetry, Phys. Rev. B **83**, 115125 (2011).

[35] B. Bauer, P. Corboz, R. Orús, and M. Troyer, Implementing global abelian symmetries in projected entangled-pair state algorithms, Phys. Rev. B **83**, 125106 (2011).

[36] I. P. McCulloch and M. Gulácsi, The non-Abelian density matrix renormalization group algorithm, EPL **57**, 852 (2002).

[37] S. Singh and G. Vidal, Tensor network states and algorithms in the presence of a global SU(2) symmetry, Phys. Rev. B **86**, 195114 (2012).

[38] B. Bruognolo, J.-W. Li, J. von Delft, and A. Weichselbaum, A beginner's guide to non-abelian iPEPS for correlated fermions, SciPost Phys. Lect. Notes , 25 (2021).

[39] P. Schmoll, S. Singh, M. Rizzi, and R. Orús, A programming guide for tensor networks with global SU(2) symmetry, Annals of Physics **419**, 168232 (2020).

[40] N. Schuch, I. Cirac, and D. Pérez-García, PEPS as ground states: Degeneracy and topology, Annals of Physics **325**, 2153 (2010).

[41] O. Buerschaper, Twisted injectivity in projected entangled pair states and the classification of quantum phases, Ann. Phys. **351**, 447 (2014).

[42] K. Duivenvoorden, M. Iqbal, J. Haegeman, F. Verstraete, and N. Schuch, Entanglement phases as holographic duals of anyon condensates, Phys. Rev. B **95**, 235119 (2017).

[43] N. Bultinck, M. Mariën, D. Williamson, M. Şahinoğlu, J. Haegeman, and F. Verstraete, Anyons and matrix product operator algebras, Annals of Physics **378**, 183 (2017).

[44] S. P. G. Crone and P. Corboz, Detecting a Z_2 topologically ordered phase from unbiased infinite projected entangled-pair state simulations, Phys. Rev. B **101**, 115143 (2020).

[45] M. B. Şahinoğlu, D. Williamson, N. Bultinck, M. Mariën, J. Haegeman, N. Schuch, and F. Verstraete, Characterizing Topological Order with Matrix Product Operators, Ann. Henri Poincaré **22**, 563 (2021).

[46] M. Fishman, S. R. White, and E. M. Stoudenmire, The ITensor Software Library for Tensor Network Calculations, SciPost Phys. Codebases , 4 (2022).

[47] J. Hauschild and F. Pollmann, Efficient numerical simulations with Tensor Networks: Tensor Network Python (TeNPy), SciPost Phys. Lect. Notes , 5 (2018).

[48] H. Zhai, H. R. Larsson, S. Lee, Z.-H. Cui, T. Zhu, C. Sun, L. Peng, R. Peng, K. Liao, J. Tölle, J. Yang, S. Li, and G. K.-L. Chan, Block2: A comprehensive open source framework to develop and apply state-of-the-art DMRG algorithms in electronic structure and beyond, J. Chem. Phys. **159**, 234801 (2023).

[49] C. R. Roberts *et al.*, Tensornetwork: A library for easy and efficient manipulation of tensor networks, `https://github.com/google/TensorNetwork`.

[50] K.-H. Wu, C.-T. Lin, K. Hsu, H.-T. Hung, M. Schneider, C.-M. Chung, Y.-J. Kao, and P. Chen, The cytnx library for tensor networks, SciPost Phys. Codebases (2023).

[51] Y. Motoyama, T. Okubo, K. Yoshimi, S. Morita, T. Kato, and N. Kawashima, Tenes: Tensor network solver for quantum lattice systems, Comput. Phys. Commun. **279**, 108437 (2022).

[52] J. Haegeman and contributors, TensorKit.jl (2024).

[53] A. Weichselbaum, QSpace - An open-source tensor library for Abelian and non-Abelian symmetries, SciPost Physics Codebases , 040 (2024).

[54] J. Hasik and contributors, peps-torch: Solving two-dimensional spin models with tensor networks (powered by pytorch), `https://github.com/jurajHasik/peps-torch`.

[55] B. Ponsioen, Sample implementation of ipeps ground-state and excitation algorithms with automatic differentiation, `https://github.com/b1592/ad-peps`.

[56] J. Naumann, E. L. Weerda, M. Rizzi, J. Eisert, and P. Schmoll, varipeps – a versatile tensor network library for variational ground state simulations in two spatial dimensions, arXiv:2308.12358 (2023).

[57] M. van Damme and contributors, PEPSKit.jl: Tools for working with projected entangled-pair states, `https://github.com/quantumghent/PEPSKit.jl`.

[58] T. Chanda, Tennetlib.jl, `https://github.com/titaschanda/TenNetLib.jl`.

[59] M. M. Rams, G. Wójtowicz, A. Sinha, and J. Hasik, Yastn: Yet another symmetric tensor networks; a python library for abelian symmetric tensor network calculations (2024), arXiv:2405.12196 [cond-mat.str-el].

[60] T. Nishino and K. Okunishi, Corner Transfer Matrix Renormalization Group Method, J. Phys. Soc. Jpn. **65**, 891 (1996).

[61] Z. Y. Xie, J. Chen, M. P. Qin, J. W. Zhu, L. P. Yang, and T. Xiang, Coarse-graining renormalization by higher-order singular value decomposition, Phys. Rev. B **86**, 045139 (2012).

[62] Similar issues arise in the SU(2) case, where transforming into the $\mathbb{Z}_2$ Hermitian basis would require to mix states $|S_{total}, S^z = k\rangle$ with $|S_{total}, S^z = -k\rangle$ in each spin sector S_{total}.

[63] We note that $(E_{sym} - E)$ is not necessarily positive, because if the non-symmetric state is not Hermitian (i.e. unphysical), it is not strictly variational. Also note that in general the contraction error itself may not be strictly variational.

[64] M. Levin and C. P. Nave, Tensor Renormalization Group Approach to Two-Dimensional Classical Lattice Models, Phys. Rev. Lett. **99**, 120601 (2007).

[65] R. Orús and G. Vidal, Simulation of two-dimensional quantum systems on an infinite lattice revisited: Corner transfer matrix for tensor contraction, Phys. Rev. B **80**, 094403 (2009).

[66] P. Corboz, T. M. Rice, and M. Troyer, Competing States in the t-J Model: Uniform d-Wave State versus Stripe State, Phys. Rev. Lett. **113**, 046402 (2014).

[67] G. Evenbly and G. Vidal, Tensor Network Renormalization, Phys. Rev. Lett. **115**, 180405 (2015).

[68] V. Zauner-Stauber, L. Vanderstraeten, M. T. Fishman, F. Verstraete, and J. Haegeman, Variational optimization algorithms for uniform matrix product states, Phys. Rev. B **97**, 045145 (2018).

[69] M. T. Fishman, L. Vanderstraeten, V. Zauner-Stauber, J. Haegeman, and F. Verstraete, Faster methods for contracting infinite two-dimensional tensor networks, Phys. Rev. B **98**, 235148 (2018).

[70] K. Homma, T. Okubo, and N. Kawashima, Nuclear norm regularized loop optimization for tensor network, Phys. Rev. Res. **6**, 043102 (2024).

[71] P. C. G. Vlaar and P. Corboz, Simulation of three-dimensional quantum systems with projected entangled-pair states, Phys. Rev. B **103**, 205137 (2021).

[72] P. C. G. Vlaar and P. Corboz, Efficient Tensor Network Algorithm for Layered Systems, Phys. Rev. Lett. **130**, 130601 (2023).

[73] A. Kshetrimayum, M. Rizzi, J. Eisert, and R. Orús, Tensor network annealing algorithm for two-dimensional thermal states, Phys. Rev. Lett. **122**, 070502 (2019).

[74] A. Kshetrimayum, H. Weimer, and R. Orús, A simple tensor network algorithm for two-dimensional steady states, Nat. Comm. **8**, 1 (2017).

[75] C. Mc Keever and M. H. Szymańska, Stable iPEPO Tensor-Network Algorithm for Dynamics of Two-Dimensional Open Quantum Lattice Models, Phys. Rev. X **11**, 021035 (2021).